

ULTIMA: Robust and Tail-Optimal AllReduce for Distributed Deep Learning in the Cloud

Ertza Warraich, Omer Shabtai^{*}, Khalid Manaa^{*}, Shay Vargaftik[†], Yonatan Piasetzky^{*}, Matty Kadosh^{*}, Lalith Suresh[‡], and Muhammad Shahbaz
Purdue University ^{*}*NVIDIA* [†]*VMware Research* [‡]*Feldera*

ABSTRACT

We present ULTIMA, a new collective-communication system for the cloud with bounded, predictable completion times for deep-learning jobs in the presence of varying computation (stragglers) and communication (congestion and gradient drops) variabilities. ULTIMA exploits the inherent resiliency and the stochastic nature of distributed deep-learning (DDL) training to work with approximated gradients, and provides an efficient balance between (tail) performance and the resulting accuracy of the trained models.

Exploiting this domain-specific characteristic of DDL, ULTIMA introduces (1) mechanisms (e.g., Transpose AllReduce, unreliable connection-oriented transport, and adaptive timeout) to improve the DDL jobs’ tail execution time, and (2) strategies (e.g., Hadamard Transform) to mitigate the impact of gradient drops on model accuracy. Our evaluation shows that ULTIMA achieves 60% faster time-to-accuracy (TTA), on average, when operating in shared environments (e.g., public cloud), and is on par with existing algorithms (e.g., Ring-AllReduce) in dedicated environments (like HPC).

1 INTRODUCTION

Synchronous distributed data-parallel training [124] is now the de-facto standard for training large-scale deep-learning models (comprising billions or even trillions of parameters) and datasets (comprising terabytes of data) that form the backbone of many mainstream enterprise applications, including computer vision [35, 45, 64, 115], natural-language processing and large-language models [24, 34, 75, 119], recommendation and prediction systems [39, 41, 51, 53, 89], and healthcare [59, 77, 87, 120]. Under this scheme, the training occurs in rounds (or epochs). Workers locally train a copy of the model on a fragment of data and then share the model updates (i.e., gradients) among themselves over the network to compute an aggregated result. The aggregate is then used to update the model locally for the next round of training. Distributed deep-learning (DDL) is, therefore, inherently a computation- and communication-intensive workload and is becoming even more so with growing model (e.g., GPT-3[24], BERT [34], LLaMA [101]), and dataset [15, 33, 98] sizes.

To train such large models, extensive efforts are underway in reducing both the computation and communication time

of DDL jobs, albeit in isolation. On the one hand, we have GPUs [97] and emerging hardware accelerators, like Tensor Processing Units (TPUs) [56], that are drastically bringing down the computation time—reducing it by 62× over the last decade [94]. While, on the other hand, we have recent proposals based on programmable switches [110] that aim at reducing the communication time by 2–5× (via in-network aggregation) [94]. Yet, when seen together, both these efforts mainly help in improving the average completion time of a deep-learning job (either by accelerating computation or communication). The vast array of system-level variabilities (e.g., device failures, OS and hypervisor scheduling, and resource contention) and network-level delays (e.g., congestion and retransmissions) still lead to long tails; hence, resulting in poor overall performance for these training jobs [67, 81, 108]. Moreover, these solutions require changes in the provider’s network, which is outside the scope of a cloud tenant.

In this paper, we make the case for ULTIMA, a collective-communication system for the cloud tenants that ensures bounded, predictable completion times for deep-learning jobs in the presence of myriad computation and communication variabilities. ULTIMA exploits the inherent resiliency and the stochastic nature of deep-learning systems to work with approximated or partial gradients and provides an efficient balance between (tail) performance and the resulting accuracy of the trained models. Others are already utilizing this characteristic of deep learning to optimize DDL hardware design (e.g., chip area [93, 121]), minimize traffic overhead [37, 74, 107], or offload certain DDL tasks to the network switches [67, 94, 110, 114]. For example, to improve communication time, ATP [67] and SwitchML [94] utilize fixed-point arithmetic to execute gradient aggregation in programmable switches, with acceptable approximation loss. Various gradient-compression schemes [37, 74, 107] employ lossy compression to reduce network traffic overhead, while limiting deviation from the achievable model accuracy. Similarly, hardware designers are incorporating approximate operations (e.g., approx. multipliers [93, 121]) in their architectures to minimize resource and energy usage—to scale to ever-increasing DDL models.

In ULTIMA, we replace the (tail-prone) deterministic, run-to-completion stages of an AllReduce collective in DDL, with

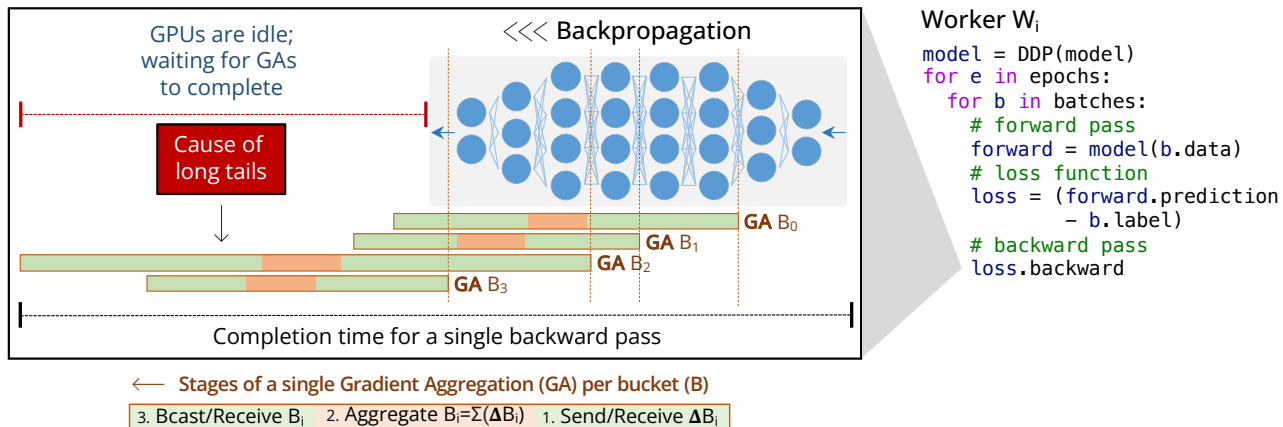


Figure 1: A backpropagation pass in distributed data-parallel (DDP) training. Multiple gradient aggregation (GA) runs share a bucket (B_i) worth of gradients among worker nodes (W_n), in parallel. The two send(bcast)/receive stages (1, 3) in GA incur the most time—contributing to the tail latency and stalling GPUs.

best-effort, *time-bounded* implementations. (1) ULTIMA introduces the notion of *Adaptive Timeouts* to restrict the time a deep-learning job spends doing computation (aggregation) and communication (gradient sharing). (2) ULTIMA implements a new *Unreliable Connection-Oriented Transport* to maximize the gradients received during each window. Unlike TCP or RDMA, which are prone to tail effects due to out-of-order delivery and retransmissions (to ensure reliability), ULTIMA implements a best-effort transport with flow- and congestion-control to deliver gradients as fast as possible within the given time window. (3) It also incorporates a *Transpose-Allreduce Collective* to further speed up gradient delivery by avoiding congested paths. (4) Finally, to minimize the impact of missed or dropped gradients, ULTIMA implements *Hadamard Transform* to ensure, for any drop pattern (e.g., tail drops), a receiver still obtains an unbiased estimate of the model’s gradients resulting in a minimal loss in accuracy.

We implement ULTIMA as a new AllReduce scheme inside Gloo [4], a popular collective-communication library. Doing so makes ULTIMA immediately compatible with existing DDL frameworks (e.g., PyTorch) without modifications. We run our experiments on various popular deep-learning models (e.g., ResNet-152 [50], VGG-19 [96], and BERT [34]) and evaluate ULTIMA under two settings: (1) a *dedicated* (non-congested, homogeneous, and lossless) environment, i.e., no packet retransmissions or stragglers, and (2) a *shared* (congested, heterogeneous, and lossy) environment, i.e., packet loss and stragglers.

Our evaluation shows that ULTIMA achieves 60% faster time-to-accuracy (TTA), on average, when operating in the shared (lossy) environment, and is on par with existing algorithms (e.g., Ring-AllReduce) in the dedicated (lossless) environment. The percentage increase in TTA between the shared

versus dedicated case for ULTIMA is within 6%; whereas, for Ring-AllReduce, it is 170%—indicating that ULTIMA yields predictable (and bounded) training times and curbs long tails. We observe that it is the latency of the gradient aggregation (GA) step (Figure 1) that inflates to 3× of the dedicated case, when operating under lossy conditions; hence, strengthening the need for a new collective like ULTIMA. We also perform a deeper analysis of the various components of ULTIMA. For example, in our evaluation, enabling Hadamard Transform mitigates the impact of tail-drops and improves TTA by 1.8× even under 10% of gradient drops.

2 BACKGROUND & MOTIVATION

We begin by providing a background on distributed deep-learning (DDL) training—more specifically, distributed data-parallel (DDP) training—and the impact of stragglers on its performance (§2.1). We then discuss existing strategies for straggler mitigation in DDL (§2.2), and make a case for a new communication-collective system, ULTIMA, that exploits the DDL’s resiliency against gradient loss for improving performance.

2.1 Distributed Deep Learning & Stragglers

Distributed deep learning (DDL) helps scale (and speedup) model training by utilizing an increasing number of hardware accelerators, e.g., GPUs [97] and TPUs [56], across server nodes [16, 26, 79]. To do so, it employs two approaches: (i) distributed data parallelism (DDP) [124] to run batches¹ on multiple accelerators in parallel, and (ii) distributed model parallelism (DMP) [57] to deploy larger models that fail to fit on a single accelerator. These approaches are orthogonal

¹A batch is a set of training data used in a given forward/backward pass.

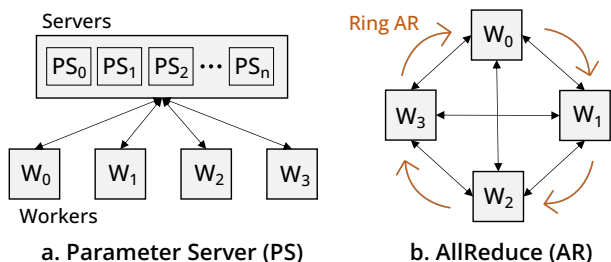


Figure 2: Architectures for gradient aggregation: Parameter Server (PS) and AllReduce (AR).

and can be used in conjunction. We focus on DDP in this paper to highlight our contributions (§3).

In distributed data parallelism (DDP), multiple worker nodes run the same deep-learning model on their portion of a training dataset, distributed evenly across nodes. Each portion is further subdivided into batches, which are processed sequentially (i.e., forward pass, loss function, and backward pass) in each epoch, Figure 1. During the forward pass, the model (e.g., a neural network) operates on a batch and generates a prediction, which is then compared with the ground truth (e.g., label) to calculate the model’s loss. Next, the backward pass computes gradients using a loss function, which is used by an optimization algorithm (e.g., Stochastic Gradient Descent, SGD [23, 60]) to update the model parameters. Finally, to ensure all workers learn from what others have learned from their portion of the dataset, these gradients are averaged (reduced) and shared across all nodes, after each backward pass.

The process of accumulating, reducing, and sharing gradients back with worker nodes is referred to as *gradient aggregation* (or reduction) [32]. Originally, reduction used to happen strictly after the backward pass; however, more recently, to hide communication latency, modern frameworks (like PyTorch [72]) overlap it with the backward pass (Figure 1). As soon as a bucket (B) worth of gradients become available on a node, it is immediately sent for reduction.²

Two common architectures for gradient aggregation are: Parameter Server (PS) [71] and AllReduce (AR) [29]. In the PS architecture (Figure 2a), a central server (or group of servers) receives (gathers) gradients from participating workers, aggregates (reduces) them, and broadcasts them back to all nodes. In AR (Figure 2b), instead of having separate servers, we distribute the aggregation task across workers, each reducing a subset of gradients and distributing them among themselves (e.g., Ring AllReduce [44, 83]). Both these architectures have their pros and cons. PS operates well in environments with less powerful worker machines but is bandwidth hungry—increasing linearly with the number of worker nodes. AR, especially Ring-AllReduce, is bandwidth

optimal but leads to longer execution delays—also increasing linearly with the number of worker nodes.

Impact of Stragglers on Performance. As shown in Figure 1, during each backward pass, all DDP worker nodes wait for the gradient aggregation (GA) operations to complete before processing the next batch of data. The forward and backward passes computation mostly take place on a machine-learning (ML) accelerator (e.g., GPU or TPU)—a highly parallel and pipelined architecture with predictable and bounded execution time [38, 109]. Therefore, it is typically the GA operations that lead to long tails and GPU stalls (taking as much as 50% of the overall DDP processing time) [94, 95]. Various factors can contribute to this slowdown in gradient aggregation, including slow workers, transmission delays, incast effects, packet loss and retransmissions, network congestion, and more. For example, in the PS architecture, each node sends a complete set of gradients to the parameter server, which can result in excessive drops and retransmissions, due to incast at the ToR switch [70, 122]—hence, increasing the time to process gradients. Similarly, in Ring AllReduce, a single slow worker (or a buggy link) can cause significant delays, because all nodes participate in the aggregation operation in the form of a ring topology.

2.2 Straggler Mitigation & Gradient Loss

Mitigating stragglers in distributed systems (as well as distributed deep learning) is an active area of research [20, 25, 30, 31, 49, 58, 91, 100, 111, 118]. One direction focuses on treating stragglers as black boxes and employs schemes, such as redundant task execution [43, 113] or skipping slow workers [28, 36, 118], to mitigate the delays due to network congestion or heterogeneous hardware, for example. They either employ backup workers and select the output of the fastest ones, or simply skip the slow workers altogether. However, the former can significantly increase the operational expense (in dollars). For example, training a GPT-3 model consisting of 175 billion parameters over 355 GPU-years (on a V100) [24] can cost an additional \$1 Million (\$5.6 Million total) on the AWS instance, p3.16xlarge, [11] with only 16% backup nodes (i.e., 2 backups for every 10 worker nodes). Whereas ignoring worker nodes entirely, in the latter case, can lead to slower convergence rates and poor accuracies [28, 118]. The other direction is to replace commodity servers with specialized hardware (e.g., powerful machines with predictable performance [117, 123]) and dedicated (loss-less) communication fabric [19, 62, 86]. Despite their success in HPC-like environments [80, 82, 85, 116], these solutions are not applicable in a cloud environment with myriads of tenants, all sharing the resources of the underlying data centers (e.g., servers and network).

²PyTorch limits these simultaneous reduction operations to two [72].

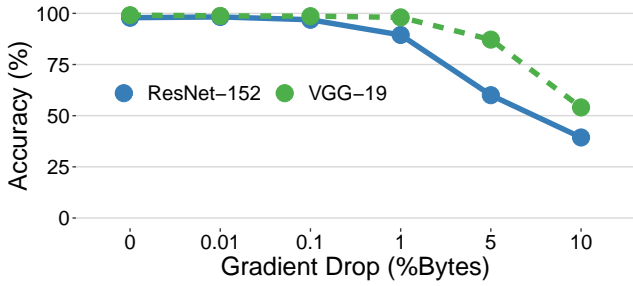


Figure 3: DDL models’ resilience to gradient drops.³

Rather than treating them as black boxes or specialized devices, we argue to replace the (tail-prone) deterministic, run-to-completion workers with their best-effort, *time-bounded* implementations. The idea is to restrict the processing time of a slow worker and utilize its partial output (gradients) in the next training phase, rather than skipping it entirely.

Resilience to Gradient Loss vs. Performance and Accuracy. Unlike traditional distributed systems (e.g., file sharing and web serving), the stochastic nature of distributed deep-learning systems provides an interesting trade-off between gradient loss (approximation or drops), performance, and accuracy. These systems (based on SGD-based optimization) [23] are shown to be resilient against estimation inaccuracies in stochastic gradients under different settings [48]. For example, various gradient sparsification [37, 90, 107] and quantization [18, 74, 108] schemes employ this fact to reduce network traffic overhead. ATP [67] and SwitchML [94] utilize fixed-point arithmetic to execute gradient aggregation in programmable switches, with acceptable approximation loss. Hardware designers incorporate approximate operations (e.g., approx. multipliers [93, 121]) to minimize chip area and energy usage. And, as shown in Figure 3, these deep-learning models are also resilient to gradient drops—sustaining high model accuracy up to 1% of gradient loss.

3 DESIGN

We present ULTIMA, a robust AllReduce communication-collective system optimized to mitigate tail-latency by exploiting the unique characteristics of distributed-deep learning (DDL), i.e., resiliency to gradient loss, to quickly reach the convergence accuracies of traditional systems (e.g., PS and Ring-AllReduce) while mitigating the impact of stragglers (slow workers) and network variabilities.

Overview. Figure 4 shows the various components of ULTIMA. *Transpose AllReduce* (§3.1) implements a peer-to-peer collective-communication fabric, where each node also serves as a parameter server (PS). *Unreliable Connection-Oriented Transport* (§3.2) lets nodes connect with each other

³We emulated drops by modifying Gloo to omit a percentage of gradients (in bytes) before sending them to PyTorch (§4).

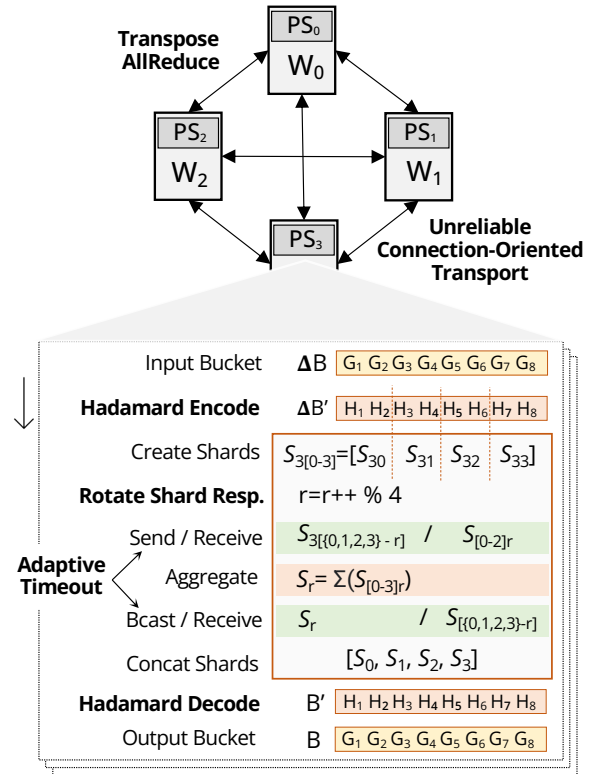


Figure 4: ULTIMA’s design: *Transpose AllReduce* with colocated parameter servers, *Unreliable Connection-Oriented Transport*, *Hadamard Transform*, *Adaptive Timeouts*, and *Rotating Shard Responsibility*.

in a best-effort but controlled manner. The parameter server (PS) on each worker node encodes (and decodes) gradients in the input bucket (B), using *Hadamard Transform* (§3.4), before creating shards (S_{ij}) of gradients to be sent to other nodes for reduction. The PS nodes iteratively *rotate shard responsibility* among themselves by maintaining a global index (r). Finally, the *Adaptive Timeout* (§3.3) bounds the time spent by the two send(bcast)/receive stages during the AllReduce phase. All these components operate in tandem to optimize for three competing objectives in ULTIMA: maximizing performance, minimizing gradient drops, and sustaining training accuracy.

3.1 Transpose AllReduce

We begin with *Transpose AllReduce* (TAR), which (a) limits the impact of slow (congested) paths during the send(bcast)/receive stages of gradient aggregation (Figure 4), and (b) sets the stage for the other design optimizations, discussed later.

As shown in Figure 5a, a congested path can severely impair the performance of Ring-AllReduce—all nodes must stall until the communication between the two nodes over the affected path finishes. And, as the same path (node pair) is used

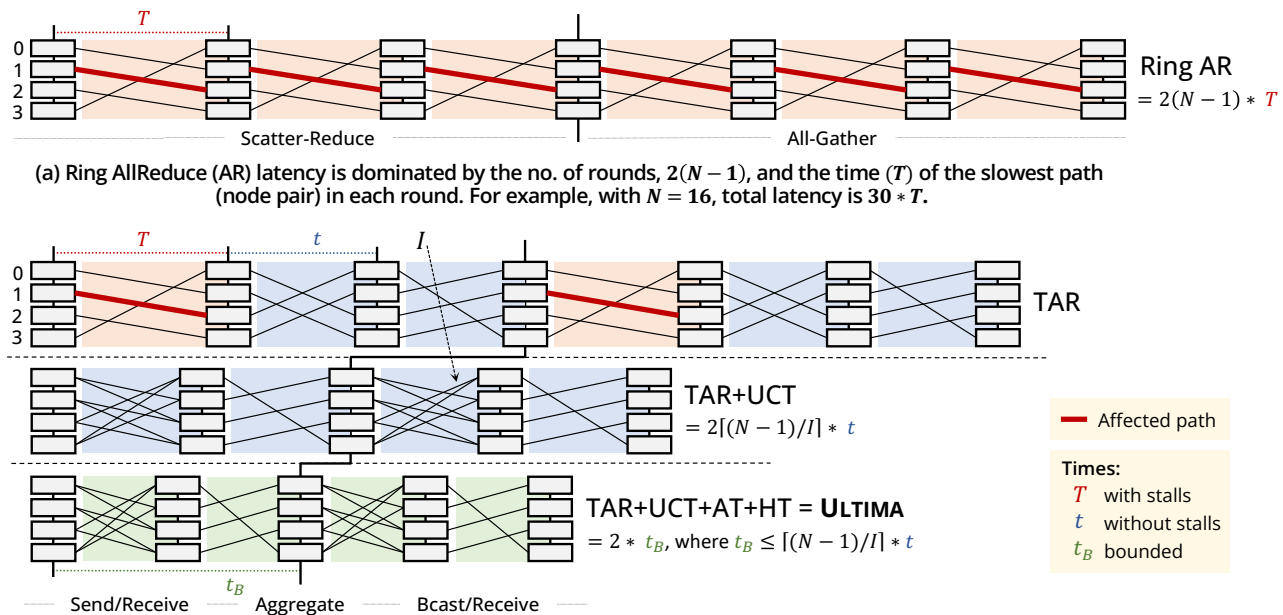


Figure 5: Ring-AllReduce versus Ultima.

in every round—a necessary condition for Ring-AllReduce [83], the latency inflates quickly with the number of worker nodes (N). For example, with T , the time taken by the affected path, the total latency for a given AllReduce phase will be $2(N-1) * T$.

Instead of picking the same path (node pair), what if we pick a different path each round? Doing so would limit the occurrences of the affected paths, resulting in faster completion times. TAR exploits this insight and implements a new collective-communication algorithm, in which a given path is picked only once—both during the send/receive and bcast/receive stages of gradient aggregation (Figure 5b: TAR); hence, limiting the impact of the affected paths to at most two rounds. The total AllReduce completion time now reduces to $2(N-2) * t + 2 * T$, where $t \ll T$.⁴

3.1.1 TAR Algorithm: A Colocated PS-inspired Collective. TAR combines the key features of both traditional AllReduce (i.e., bounding path occurrences using Peer-to-Peer, P2P, communication) [29, 69] and Ring-AllReduce (i.e., minimizing bandwidth using shards and avoiding incast via rounds) [83].

In TAR, each node acts as a worker as well as a parameter server (PS), connected together over a peer-to-peer (P2P) collective-communication fabric (Figure 4). Each PS node (PS_i) receives a bucket of gradients (ΔB) as input from the worker process (W_i) and divides it into N shards ($S_{i[0..N]}$),

⁴When $T \rightarrow t$, TAR and Ring-AllReduce perform similarly (§5).

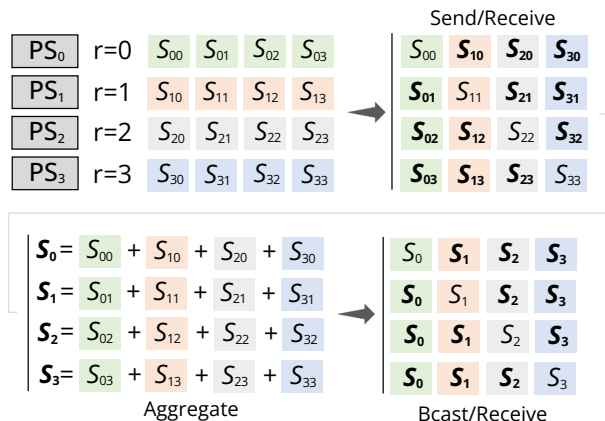


Figure 6: Transpose AllReduce algorithm: PS nodes send/receive shards S_{ij} , aggregate them, and bcast/receive to other nodes (all acquiring the same copy).

equal to the number of nodes. It keeps the shard S_{ir} , it is responsible for aggregating, and sends the remaining shards ($S_{i[\{0..N\}-r]}$) to the neighboring nodes. At the same time, PS_i waits for its shards ($S_{[\{0..N\}-i]r}$) and aggregates (i.e., averages) them with S_{ir} into a single shard S_r . Next, it broadcasts S_r to all nodes and receives the aggregated shards from them, $S_{[\{0..N\}-r]}$. Finally, these shards are concatenated into a bucket (B) and forwarded to the worker (W_i) to process the next batch of data. When $r=i$, the whole operation appears like a row-wise sum of the transpose of the shard matrix S , as shown in Figure 6; hence, the name *Transpose AllReduce*.

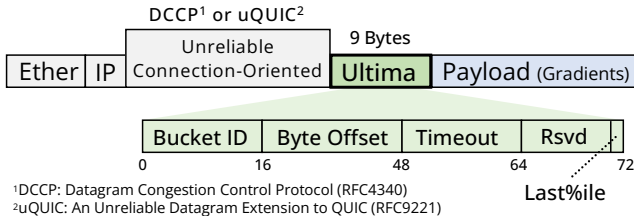


Figure 7: ULTIMA’s transport header format

In P2P, each PS node communicates directly with the other nodes (instead of forming a ring). When sharing gradients, they all interact with each other twice: once sending/receiving shards to the other node and then broadcasting/receiving aggregated shards, hence limiting the impact of the affected paths (node pairs). Sharding also alleviates the load on the PS nodes, where each node only aggregates a bucket (B) worth of gradients (rather than $N * B$).⁵ Moreover, TAR utilizes the same bandwidth as Ring-AllReduce by sending $B * (N - 1)$ bytes over the network during the two send(bcast)/receive stages. Lastly, to mitigate incast, TAR splits the communication between PS nodes over multiple rounds, where—unlike Ring-AllReduce with fixed paths (Figure 5a)—nodes communicate with each other using a round-robin strategy,⁶ ensuring a given path (node-pair) never repeats across rounds (Figure 5b: TAR).

Summary. TAR behaves similarly to Ring-AllReduce but *reduces latency by limiting the occurrences of the affected paths*. Next, we discuss how to improve these affected paths, themselves, and to reduce the number of rounds using a new transport architecture (§3.2).

3.2 Unreliable Conn.-Oriented Transport

One of the primary causes affecting paths (node pairs) is the variability in the network behavior, due to retransmissions and congestion [31]. Current connection-oriented protocols (like TCP) further exacerbate these effects by demanding reliable, in-order delivery of packets (gradients) between PS nodes—if packets are dropped or received out-of-order, TCP will stall until all gradients are received over the affected path.

What if we disregard these packets and their order and continue ahead? Nodes can then move quickly by processing the gradients they received without waiting, thus mitigating the impact of the affected paths (i.e., $T \rightarrow t$, Figure 5b: TAR+UCT). As shown in Figure 3, DDL models are resilient to such packet loss, and our evaluations (§5) further confirm that these models can sustain full model accuracies despite these dropped gradients.

⁵PyTorch and TesnorFlow typically use a bucket size of 25 MB [72, 92].

⁶We leave exploring other load-sharing strategies as future work.

However, replacing TCP with message-based protocols (like UDP) would not work. UDP is fast, as it does not retransmit packets or reorder them, but it also does not perform congestion or flow control. It sends all data at link speed (e.g., 40 Gbps)—causing excessively more drops (loss of gradients) in the network than what the DDL model can sustain.

3.2.1 ULTIMA’s Transport Protocol. We need a transport protocol that implements congestion and flow control but does not provide reliable, in-order delivery. Fortunately, the Linux kernel already supports such a protocol since v2.6.14 [8], called Datagram Congestion Control Protocol (DCCP) [63]. And, more recently, RFC9221 adds “support for sending and receiving unreliable datagrams over a QUIC connection” [84]. These protocols support congestion control (with ECN) as well as flow control, and provide an unreliable, connection-oriented transport (UCT) semantic to avoid the arbitrary delays associated with TCP.⁷

ULTIMA extends these protocols by adding a new 9-byte header, *Ultima* (Figure 7), to commit arriving packets (with gradients) to the right bucket and offset using the header fields, *Bucket ID* and *Byte Offset*, respectively. These fields ensure that gradients reach the correct bucket, irrespective of the ordering of the incoming packets when multiple GA operations are running in parallel (Figure 1).

3.2.2 Incast Factor (I). ULTIMA also introduces a notion of an incast factor I (Figure 5). By varying I , the TAR’s P2P communication model lets ULTIMA alter the number of senders a PS node can receive gradients from in a given round. For example, setting $I = 1$ would cause TAR to take the same number of rounds as Ring-AllReduce, $2(N - 1)$; however, increasing $I = 2$ would quickly reduce these rounds by about half, $2\lceil(N - 1)/2\rceil$; and so on. A user can configure the incast factor (I), as another parameter, based on the available node capacity—allowing GA operations to finish in fewer rounds.

Summary. UCT, in conjunction with TAR, *minimizes the latency of the affected paths*, while the incast factor (I) helps reduce the number of rounds.

3.3 Adaptive Timeout

We now introduce Adaptive Timeout (AT) to limit the tail communication time of the send(bcast)/receive stages of the GA operations to t_B (Figure 5: TAR+UCT+AT+HT). TAR+UCT minimizes latency but is still prone to tail effects due to congestion (and stragglers). Thus, by restricting the time to t_B , we can control the worst-case execution of these stages—allowing GA operations to finish in a bounded time.

However, there are a couple of challenges with this approach. (1) How to select the value of t_B ? Too small will lead

⁷We consider these protocols (e.g., DCCP) for their convenience and availability, but understand that more robust implementations are possible (e.g., RDMA-based) [47]. We hope to explore those as future work.

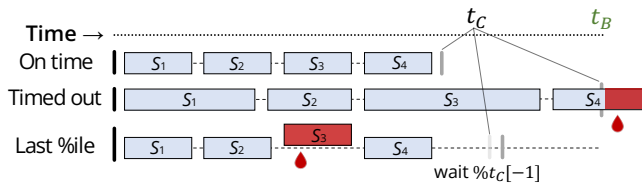


Figure 8: Different timeout strategies in ULTIMA.

to undue loss, and too high will cause unnecessary delays. Moreover, the value will vary with environmental settings (e.g., GPU type, CPU clock, vCPUs, and interface speed) and parameters (e.g., no. of nodes, bucket sizes, and incast factor). (2) A single lost packet, which is likely in UCT, would cause the GA operation to always take t_B (worst-case) time to finish. TCP, on the other hand, can perform better in some instances where communication may finish faster than waiting for the full timeout (t_B), even with retransmissions.

3.3.1 Selecting the Timeout Value (t_B). As shown in Figure 1, during backpropagation, multiple GA operations execute in parallel on buckets of varying sizes. For selecting t_B , during the initialization phase, we run GA with TAR+TCP, using the largest bucket, for a couple of iterations to collect completion times for both send(bcast)/receive stages.⁸ PS nodes share these values with each other using the Timeout field in the ULTIMA header (Figure 7).

We then form a list of these times and set t_B to the 95th %ile of that list. In §5, we show that using 20 iterations and the 95th %ile value allows ULTIMA to sustain full model accuracies while finishing 3x faster.

3.3.2 Progressing Quickly via Early Timeout. To avoid approaching t_B every time a loss happens, we introduce an early timeout strategy, which causes GA receive stages to expire whenever there are no remaining gradients to read (i.e., the buffer is empty). For each bucket, we maintain a moving average (t_C) of completion times; we keep separate averages for both the receive stages in GA (Figure 5). The sender PS node tags the last 99th %ile packets by setting the Last%ile field in the header. When the buffer is empty, the receiver node checks if some of the last %ile packets have been received from all nodes. If so, it waits for an $x\%$ of t_C time before expiring (Figure 8).

We calculate t_C in the following steps. First, we compute the (expected) completion time of a given receive stage: (1) if on time, then we set t_C to the current time spent, (2) if timed out, then $t_C = t_B$, and (3) if last %ile received, then t_C is set to the expected time needed to receive all data (e.g., $t_C = \text{current time spent} \times \text{total} / \text{received data}$). Next, we calculate the moving average: $t_C = \alpha * t_C + (1 - \alpha) * t_C[-1]$. Finally, we pick the median t_C from the values computed by the N PS nodes (shared over the Timeout field in the header).

⁸TCP ensures all data is sent/received during each run.

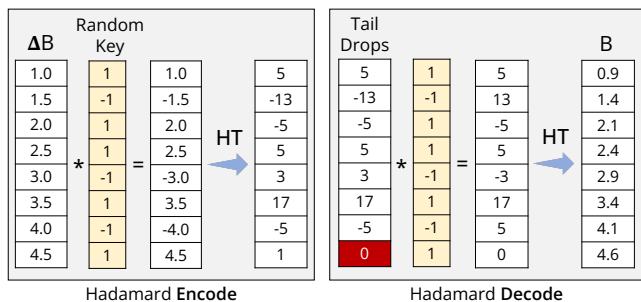


Figure 9: Dispersing the effect of lost gradients (e.g., due to tail drops) using Hadamard Transform (HT).

Summary. AT, with TAR+UCT, bounds the communication latency of the send(bcast)/receive stages in GA, further curtailing tail.

3.4 Hadamard Transform

Finally, to make ULTIMA resilient against drop patterns (e.g., tail drop) in the network, we employ *randomized* Hadamard Transform (HT) [99, 102, 103], which spreads the effect of a dropped gradient over the entire bucket. For example, in Figure 9, HT encodes a bucket (ΔB) and sends it over the network. Upon reception, the last gradient (in red) was lost (e.g., due to tail drop); however, HT preserves the lost information by slightly perturbing the values of other gradients in the decoded bucket (B). The Mean Squared Error (MSE) between the decoded and received (without HT) bucket, compared to the original one, is 0.01 and 2.53, respectively. That is why, when combined with rotating shard responsibility between nodes, HT lets ULTIMA be more aggressive with the timeout value (t_B) while still reaching high model accuracies.

3.4.1 Randomized HT. In randomized HT, a uniform random rotation (i.e., key) is applied to the incoming bucket before encoding, which results in an unbiased estimate of the gradient for any drop pattern [102]. All coordinates of the rotated gradient vector follow the same distribution, therefore dropping any particular subset results in the same distribution of the reconstructed vector after the inverse rotation. Similarly, a summation operation in HT, when applied to the encoded buckets, yields the same outcome upon decoding as the original buckets, i.e., $H(X) + H(Y) \rightarrow H(X + Y) \rightarrow H'(X + Y) == X + Y$. Moreover, randomized HT admits an efficient in-place GPU implementation [40] with minimal computation overhead.

Summary. HT, together with TAR+UCT+AT, limits the effect of dropped gradients by spreading it across the entire bucket, thus preserving the lost information. Additionally, it allows ULTIMA to operate faster, with stringent t_B values, without affecting convergence accuracies (§5).

4 IMPLEMENTATION

We develop ULTIMA as a new collective-communication scheme inside the Gloo library (v0.5.0) [4] and integrate it with PyTorch Distributed (v1.12) [72], a widely used deep-learning framework—allowing ULTIMA to work without modification with a large body of deep-learning models (e.g., CNNs [50, 66, 96], RNNs [27, 52, 78], and Transformers [24, 34, 104]).

We extend the C++ implementation of Gloo to support our Transpose AllReduce (TAR) collective and provide support for both reliable transport (over TCP) and our best-effort transport, which is a simplified version of UCT (over UDP), using the Nvidia DDPK API (v20.11) [3]. We further add support for communication hiding in ULTIMA, i.e., running two AllReduce operations in parallel with backpropagation.⁹ The sender maintains separate layer-3 (UDP) port numbers to tag gradients for the two parallel AllReduce operations. On the receive side, two PMD threads poll incoming traffic (gradients) in their local receive queues. An Nvidia Connectx-6 NIC routes traffic to the respective queues based on the port numbers; we install rules in the NIC using DDPK’s `rte_flow` API [2]. We also install rules to route non-ULTIMA traffic to the kernel using DDPK’s Flow Bifurcation mechanism [1].¹⁰ Doing so ensures that Gloo’s kernel stack remains unaffected and other network operations, e.g., rendezvous operation in PyTorch DDP [72], continue uninterrupted.

To implement Adaptive Timeouts, we use C++’s `wait_for()` function [55], which is a blocking call that returns either when a given condition is met (such as received all gradients) or a timeout occurs. For the timeout, we pair the `wait_for()` function with Chrono library’s `high_resolution_clock()` [55] to operate at nanosecond clock granularity. For Hadamard Transform, we apply a widely-used C++/CUDA implementation by HazyResearch [5], which uses GPUs to perform this operation. We use PyTorch DDP’s communication hook [13] to register Hadamard’s encode/decode callbacks for processing gradient buckets before and after reduction, respectively.

5 EVALUATION

In this section, we provide an end-to-end comparison of ULTIMA with state-of-the-art solutions (§5.2), and microbenchmark the utility of various design components (§5.3).

5.1 Experimental Setup

Testbed Environment. Our test environment is a collection of four servers configured as a Proxmox VE cluster [12] (Figure 10). Each machine has a 64-core Intel Xeon Platinum 8358P CPU @ 2.60GHz, 512 GB RAM, and an Nvidia

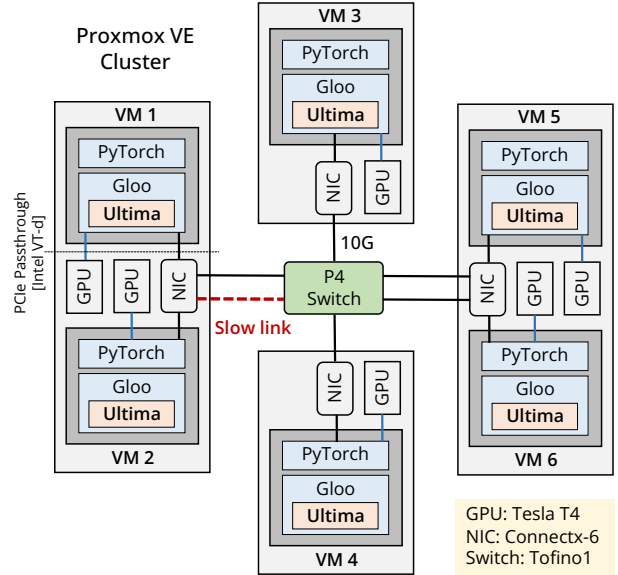


Figure 10: Our testbed: a Proxmox VE cluster with four servers hosting six VMs (running PyTorch/Gloo/Ultima), each having a Tesla T4 GPU and a dedicated network interface using Intel’s VT-d PCIe passthrough technology, and connected using a P4 Tofino switch. A slow link in red induces drops during experiments.

Connectx-6 dual-port NIC. In total, there are six Nvidia Tesla T4 GPUs, for each VM in the cluster. The VMs communicate over the network using a dedicated NIC port with Nvidia’s OFED device drivers (v5.7). Both GPU and NIC interfaces are exposed to the VMs via Intel’s VT-d PCIe passthrough technology [17]—allowing direct (dedicated) access to the physical functions. An Intel’s P4 Tofino1 switch [6] connects the servers (and VMs) using a 10 G fabric. To emulate a slow link, we randomly drop packets on the link between the switch and VM 2 based on a packet loss probability, P_{loss} . For each arriving packet, we enforce the drop policy in P4 by computing a random number n between 0 and N (where N is a very large value). We then compare it with $M = N * P_{loss}$; if $n < M$, we mark the packet to drop, and let it pass otherwise.

Baselines, Workloads, Parameters, and Evaluation Metrics. We evaluate ULTIMA against two state-of-the-art solutions, Ring-AllReduce, and Bcube-AllReduce. We also compare with a reliable version of our Transpose AllReduce (TAR) with TCP (TAR+TCP). We use a combination of compute-intensive (ResNet-152 [50]) and network-intensive (VGG-19 [96]) deep-learning models, as well as a transformer-based large-language model (BERT [34]) in our end-to-end experiments. For the ResNet model, we use the Tiny ImageNet dataset, containing 100 K images of 200 classes. The VGG model uses the CIFAR-100 [65] dataset with 60 K images divided into 100 classes. The BERT model is trained on

⁹This is consistent with existing parallelism approaches that allow for two concurrent AllReduce operations (e.g., PyTorch [72]).

¹⁰Flow Bifurcation is a mechanism that lets hardware-capable NICs forward traffic directly to the userspace (DPDK thread) or the Linux kernel.

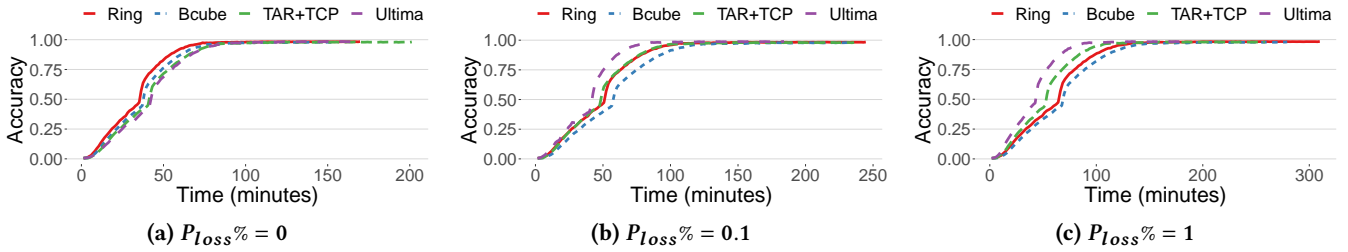


Figure 11: Time-to-accuracy (TTA) of baseline systems vs ULTIMA for ResNet-152.

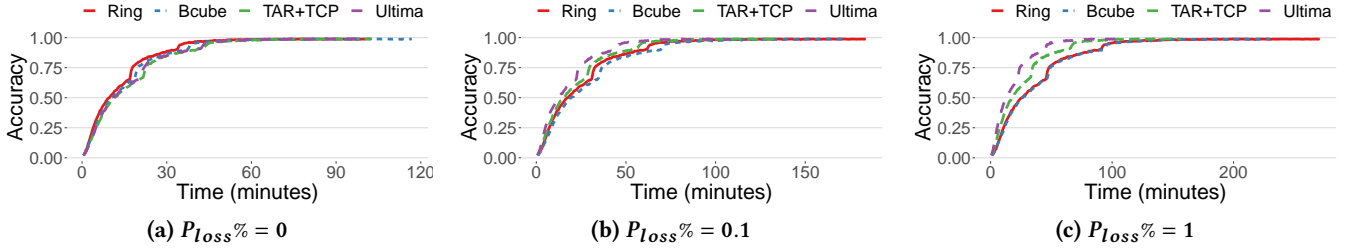


Figure 12: Time-to-accuracy (TTA) of baseline systems vs ULTIMA for VGG-19.

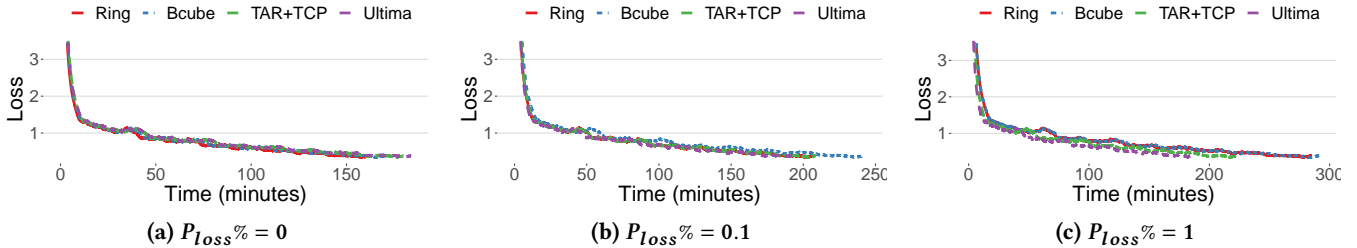


Figure 13: Time-to-loss (TTL) of baseline systems vs ULTIMA for BERT.

Scheme	TTA (minutes)				Dropped Gradients (%Bytes)				Convergence Accuracy (%)			
	0	0.01	0.1	1	0	0.01	0.1	1	0	0.01	0.1	1
Ring	100	116	184	271	—	—	—	—	99.014	99.014	99.014	99.014
Bcube	+17	+6	-13	-41	—	—	—	—	-0.12	-0.12	-0.12	-0.12
TAR+TCP	+2	-4	-50	-115	—	—	—	—	+0.169	+0.169	+0.169	+0.169
ULTIMA	-1	-14	-77	-166	0.00009	0.0003	0.02	0.08	+0.132	+0.008	+0.072	+0.051

Table 1: Comparing end-to-end training of baseline systems vs ULTIMA on VGG-19 (total gradients 3.5 TB).

SQuAD2.0 [88] dataset, which contains 150,000 questions for text comprehension and question/answering. We also use the Lenet-5 [68] model for one of the microbenchmarks and pair it with the FashionMNIST [112] dataset, which contains 60 K images across 10 classes. We compute the ULTIMA’s timeout value (t_B) for each model using 20 iterations; we set $\alpha = 0.95$ when calculating the moving average (t_C) and wait for 10% of t_C before expiring.

For end-to-end training experiments (§5.2), we employ the time-to-accuracy (TTA) metric for ResNet and VGG models, which measures the time required to achieve a specific accuracy threshold. Whereas for BERT, we opt for the time-to-loss

(TTL) metric. We calculate TTL by computing a rolling average of the model’s loss across 100 training steps for any given point in time. For microbenchmarks (§5.3), we measure the impact of each of the ULTIMA’s design components on gradient loss, performance (in terms of latency), and model accuracy.

5.2 End-to-End Evaluation

We perform our end-to-end evaluation over a range of network conditions for $P_{loss}\% = 0$ to 1, using the three models: ResNet-152, VGG-19, and BERT. We compare ULTIMA, with the incast factor $I = 1$, against the three baseline systems

(Ring, Bcube, TAR+TCP) and measure their time-to-accuracy (TTA) for the image classification tasks and time-to-loss (TTL) for an NLP task. We also measure the percentage of gradients dropped (in bytes) and the achieved training accuracy (loss). Our evaluations show that ULTIMA outperforms the baseline systems, achieving up to 60% reduction in TTA/TTL, on average, under varying congestion settings ($P_{loss}\%$ = 0, 0.01, 0.1, and 1). It maintains the same convergence accuracy (and loss) as the baselines while keeping the lost gradients to less than 0.02%, on average, of the communicated traffic.

TTA and Convergence Time. Figure 11–13 show how TTA/TTL of the three baselines and ULTIMA change as the value of $P_{loss}\%$ increases for all three models, ResNet-152, VGG-19, and BERT models. For $P_{loss}\%$ = 0 (i.e., no congestion), Ring maintains a higher TTA value as the experiment starts. For example, at the 30-min mark, the VGG-19’s accuracy is 89% for Ring, whereas it’s 85% for ULTIMA. Other systems (Bcube and TAR+TCP) also perform similarly well compared to ULTIMA. This is because the added overhead of adaptive timeouts in ULTIMA increases its epoch completion time (e.g., by 15%) compared to baseline systems. However, all systems (including ULTIMA) typically reach the final convergence accuracy (99% for VGG-19) at about the same time (i.e., 100 mins)—as stragglers start to overwhelm the baselines, which ULTIMA mitigates.

For $P_{loss}\%$ = 0.1 and higher, the network congestion (and stragglers) start to inflate the epoch processing time for the baselines, causing them to take as high as 2× more time (e.g., 271 mins for VGG-19 on Ring) to reach the final convergence accuracy (Table 1). ULTIMA, on the other hand, retains its TTA value (i.e., 105 mins for VGG-19), while achieving similar convergence accuracy (99%), Table 1.

Gradient Drops and Convergence Accuracy. We further evaluate the drops in gradient data and their impact on convergence accuracy as we increase the $P_{loss}\%$ value (Table 1). We see that for $P_{loss}\%$ = 0, a small percentage of gradient data is lost (e.g., 0.0009%) due to ULTIMA’s timeout, causing the system to progress without waiting on the stragglers. (These timeouts manifest as dropped gradients in ULTIMA; whereas baseline systems stall on these stragglers). Still, ULTIMA achieves the same convergence accuracy (99% for VGG) as the baselines. Increasing $P_{loss}\%$ to higher values causes more gradient data to be lost, due to increased congestion in the network, but only slightly (0.08% for $P_{loss}\%$ = 1); and does not impact ULTIMA’s training accuracy.

5.3 Microbenchmarks

We now evaluate the effectiveness of the individual design components in ULTIMA. We run the VGG-19 model with the CIFAR-100 dataset for these measurements unless stated otherwise.

Reduction Scheme	MSE
Ring AllReduce (AR)	14.55
Parameter Server (PS)	9.90
Transpose AllReduce (TAR)	2.47

Table 2: Mean Squared Error (MSE) of different reduction schemes using UCT with $P_{loss}\%$ = 0.1.

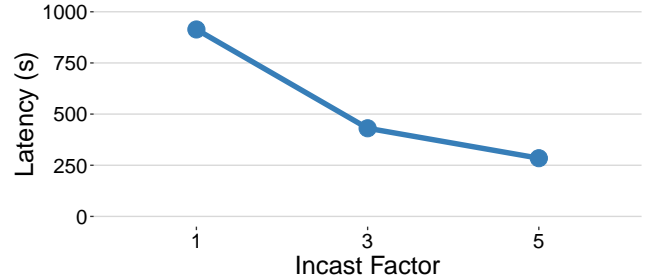


Figure 14: Training latency for Lenet-5 in ULTIMA with increasing incast factor (I).

x% of t_C	Dropped Gradient (%Bytes)	Latency (ms)
1	0.99300	230.52
5	0.07800	242.45
10	0.00009	254.36
20	0.00000	279.48

Table 3: Tradeoff between latency and dropped gradients when varying the wait time (x% on t_C) during last%ile using VGG-19 with six nodes.

ULTIMA’s TAR topology leads to minimum dropped gradients when using a best-effort transport. We compare the number of gradients lost using different AllReduce topologies with an unreliable, connection-oriented protocol (like UCT). We measure Mean Squared Error (MSE) to gauge the difference between the original gradients and the ones received over these topologies. Table 2 shows MSE for three different schemes under $P_{loss}\%$ = 0.1: Ring topology in Ring-AllReduce, P2P in PS, and P2P with rounds in TAR. Ring-AllReduce has the worst MSE (of 14.55)—an order of magnitude more than TAR. The presence of the affected path (§3.1) during each round in Ring-AllReduce leads to more losses compared to TAR. PS also exhibits high MSE (of 9.92), which is due to the incast happening when all nodes share their gradients with the parameter server at once. TAR avoids that by distributing communication over rounds while limiting the occurrence of the affected path.

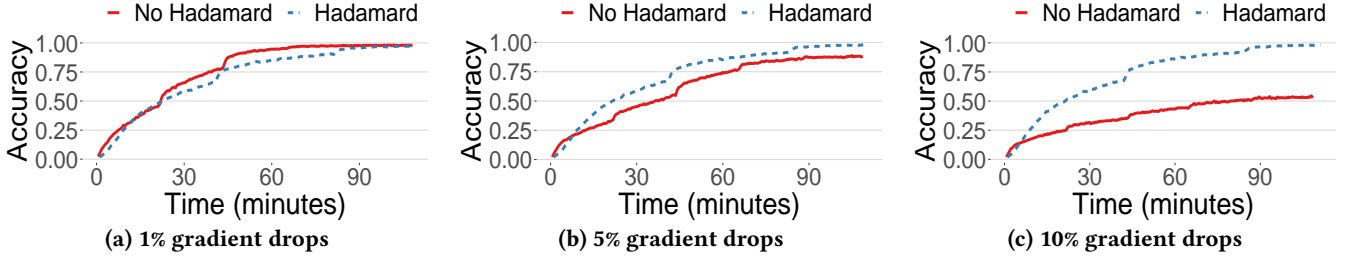


Figure 15: Training accuracy of VGG-19 with/without Hadamard Transform (HT).

ULTIMA’s incast factor (I) improves latency without overburdening the receiver nodes. Figure 14 shows how varying the incast factor (I) in ULTIMA, affects the training latency of Lenet-5 (convergence accuracy is maintained across runs). Increasing I from 1 to 3 reduces latency by about half (913.71s to 430.88s), and brings it down even further to 284.56s when $I = 5$. Having this control over the incast factor (I) allows ULTIMA to configure itself based on the capacity of the server resources, which is not the case with PS (all workers send to parameter server) or Ring-AllReduce (a receiver interacts with a single sender in a round).

ULTIMA’s early timeout strategy enables faster progress towards TTA. We also evaluate the effectiveness of the early timeout strategy (t_C) in ULTIMA. We disable t_C and only keep the timeout value t_B and measure its effect on training accuracy, latency, and dropped gradients. We find that when training VGG-19 with $P_{loss}\% = 0.1$, ULTIMA takes 127 minutes to reach convergence accuracy while incurring 0.02% of gradient drops. Enabling early timeout brings this latency down by about 16% (to 107 minutes) with a similar drop rate (0.02%). By adapting t_C , ULTIMA sustains the same drop rate and finishes quickly, rather than waiting for the higher t_B value each time. We also notice that with early timeout enabled, ULTIMA triggers t_C 95% more often than t_B ; hence, resulting in faster TTAs.

Another key parameter in our early timeout strategy is the wait time ($x\%$ of t_C). It is time we wait before expiring when no new gradients are arriving and ULTIMA has received last- $x\%$ ile gradients from all nodes (Figure 8). Table 3 shows how varying this parameter impacts latency and gradient drops. Too small ($= 1$) causes ULTIMA to miss delayed gradients and increases the drop rate to 0.993%. Increasing it to higher values ($= 5, 10$) reduces gradient drops by orders of magnitude but at the cost of higher latencies (+12 ms and +24 ms, respectively). Setting it to an even higher value ($= 20$) results in no drops but has the highest latency of 279.48 ms.

We see that t_B and wait time ($x\%$ of t_C) directly impact the end-to-end performance of ULTIMA by trading off latency and lost gradients. Care must be taken in setting these values, as they vary from environment to environment. We can

compute t_B through profiling, and wait time can be set based on user preference, e.g., choosing latency over drops.

ULTIMA’s Hadamard Transform (HT) allows it to reach convergence accuracies even under higher percentages of dropped gradients. Figure 15 shows the training accuracy of VGG-19 model with (and without) Hadamard enabled. Considering TTA, we see that Hadamard has some computational overhead when operating with only 1% of dropped gradients (Figure 15a). It takes Hadamard more time to reach convergence accuracies (around 97 minutes) compared to when it is disabled (90 minutes). However, as drops increase (5% or more), it starts to outperform the non-Hadamard instance with much faster TTAs (Figure 15b,c). Looking closely, we notice that across all dropped percentages, Hadamard is able to sustain the same TTA (≈ 97 minutes)—showing its resilience to drops. In contrast, the non-Hadamard case quickly degrades and is not able to achieve convergence accuracy under 10% drops at all. The percentage drops include both drops incurred due to network variabilities (e.g., congestion and retransmissions) and the gradients that the slow worker was not able to send due to timeouts in the first place.

6 LIMITATIONS & FUTURE WORK

Accelerators for Reduction. In ULTIMA, we primarily focus on bounding the execution time of the two send/receive stages in AllReduce (Figure 1). The reduction stage, i.e., the process of averaging gradients together still happens on CPUs. However, as models grow and gradient sizes increase, the reduction stage can become a bottleneck. Rather than opting for the most extreme case of offloading all of AllReduce to network switches, we can instead consider offloading the reduction operation on the end-host server (similar to how we accelerate GEMMs using GPUs) [97]. Modern SmartNICs [7, 9, 10], with onboard FPGAs and ML accelerators, can provide an interesting opportunity for accelerating reduction. But, doing so requires rethinking and redesigning of the application interface (API) between ULTIMA and SmartNICs. We hope ULTIMA to serve as a stepping stone for research in this direction.

Accelerators for Transport (Congestion and Flow Control). As with reduction, network transport can also become

a bottleneck with link/interface speeds reaching 400 Gbps+. Existing offloads, like RDMA [47], provide high-bandwidth communication between nodes by moving data to/from the main memory and the network without engaging the host CPU. However, these implementations are still susceptible to tail effects in the network (e.g., packet drops and retransmissions). We hope ULTIMA’s transport design can provide guidance in building new offloads for network transport, with support for unreliable, connection-oriented protocols. As a next step, we can explore RMDA’s Unreliable Connected (UC) or Unreliable Datagram (UD) queue pairs [22] to approximate and offload ULTIMA’s transport on hardware. We leave this as future work.

Dataset Over-Subscription. Despite rotating the shard responsibility among worker nodes, DDL training can still struggle to learn from the gradients being reduced at the slow worker (which were never sent due to timeouts in ULTIMA). One way to overcome this issue would be to over-subscribe the dataset fragment being processed at each node, i.e., we let the fragments overlap. That way multiple nodes get to train on a given portion of the dataset and DDL training can continue to learn from those fragments, as others will share the learned gradients when a given worker slows down. However, this may lead to redundant processing at each worker node, as they all will be processing some overlapping portions of the dataset. Another approach would be to monitor which dataset fragment is being missed often during DDL training and then reprocess that fragment again (e.g., on a backup or a spare worker).

7 RELATED WORK

Architectures for Accelerating Allreduce Collectives. Parallax [61] leverages the sparsity in model parameters to optimize DDP training. It combines AllReduce with PS to efficiently transfer data based on the observed sparsity. DLCP [106] employs packet-level prioritization and drops based on model layers and magnitudes of gradients. It uses inter-packet order-independency to further balance per-packet load across the network by giving higher priority to packets based on specific layers and magnitudes of gradients to speedup training. BytePS [54] exploits spare CPU and bandwidth resources to accelerate tasks running on GPUs. It provides a communication framework to split the functionalities of a parameter server and introduces a common summation-service abstraction (SSA) for aggregating gradients, which optimizers can accelerate using AVX instructions. HiPress [21] presents a compression-aware gradient synchronization architecture (CaSync) for DNN training; part of a gradient compression toolkit (CompLL) that reduces bandwidth using techniques, such as quantization and sparsification. A recent work, OmniReduce [37], introduces a

concept of a streaming aggregation, which exploits parameter sparsity to maximize effective bandwidth use by sending only non-zero data blocks. ULTIMA captures DDL’s resiliency to gradient drops and introduces a new Transpose AllReduce scheme and best-effort, connection-oriented transport to mitigate stragglers while sustaining convergence accuracies. It can employ techniques from past work (like OmniReduce) to minimize network usage for models with sparse gradients or utilize quantization and sparsification techniques similar to HiPress.

Accelerating Deep Learning using In-Network Computing. SHARp [46] is a hierarchical aggregation protocol and architecture in Nvidia Switches (e.g., IB-2 [14]), which builds an overlay reduction tree for aggregating data flowing through the switch. iSwitch [73] accelerates distributed reinforcement learning by moving the gradient aggregation from server nodes into FPGA-based programmable switches (e.g., NetFPGA [76]). MLfabric [105] is a contention-aware fabric designed for accelerating multi-tenant distributed training by managing communication (gradient and model transfers), delivery order, and transfers. It opportunistically aggregates updates at idle worker nodes and uses replication for fault tolerance. SwitchML [94] accelerates distributed training by using a programmable data-plane device (e.g., Intel Tofino [6]) to aggregate the model updates from multiple workers in the network. To overcome the switch memory and computational constraints, they co-design the in-switch processing with end-host protocols (e.g., sliding window of parameters) for handling drops. PANAMA [42] is a custom in-network hardware accelerator for floating-point gradient aggregation. It accompanies a load-balancing and congestion control protocol for running ML data-parallel jobs. ATP [67] is an in-network aggregation solution similar to SwitchML, but for multi-tenant learning, and is designed to provide a dynamic, best-effort in-network aggregation service for multi-tenant multi-switch clusters. Unlike these solutions, ULTIMA does not require specialized hardware and can operate over existing network fabrics in the cloud.

8 CONCLUSION

ULTIMA leverages distributed-deep learning’s (DDL) resiliency to lost gradient and achieves a speedup of 60%, on average, over state-of-the-art frameworks (e.g., Ring-AllReduce and Bcube-AllReduce) in shared (congested) and dedicated (lossless) environments. ULTIMA implements a domain-specific peer-to-peer Transpose Allreduce collective-communication algorithm and a best-effort transport protocol that outperforms existing approaches in terms of (tail) performance (i.e., TTA), without sacrificing DDL models’ convergence accuracies while keeping the gradient drops to the minimum (i.e., less than 0.02% on average).

REFERENCES

- [1] DDPK Flow Bifurcation Guide. https://doc.dpdk.org/guides-20.11/howto/flow_bifurcation.html. Last accessed: 09/2023.
- [2] DDPK Generic Flow API. https://doc.dpdk.org/guides-20.11/prog_guide/rte_flow.html. Last accessed: 09/2023.
- [3] DDPK v20.11. <https://doc.dpdk.org/guides-20.11/>. Last accessed: 09/2023.
- [4] GLOO Communication Library. <https://github.com/facebookincubator/gloo>. Last accessed: 09/2023.
- [5] HazyResearch's Hadamard CUDA Implementation. <https://github.com/HazyResearch/structured-nets>. Last accessed: 09/2023.
- [6] Intel Tofino series P4-programmable Ethernet Switch. <https://www.intel.com/content/www/us/en/products/details/network-io/programmable-ethernet-switch/tofino-series.html>. Last accessed: 09/2023.
- [7] Intel® FPGA SmartNIC . <https://www.intel.com/content/www/us/en/products/details/fpga/platforms/smartnic.html>. Last accessed: 09/2023.
- [8] Linux v2.6.14. https://kernelnewbies.org/Linux_2_6_14. Last accessed: 09/2023.
- [9] napa:tech; SmartNICs . <https://www.napatech.com/products/>. Last accessed: 09/2023.
- [10] NVIDIA ConnectX SmartNIC . <https://www.nvidia.com/en-us/networking/ethernet-adapters/>. Last accessed: 09/2023.
- [11] OpenAI's GPT-3 Language Model: A Technical Overview. <https://lambdalabs.com/blog/demystifying-gpt-3>. Last accessed: 09/2023.
- [12] Proxmox Virtual Environment. https://pve.proxmox.com/wiki/Main_Page. Last accessed: 09/2023.
- [13] PyTorch DDP Communication Hook. https://pytorch.org/docs/stable/ddp_comm_hooks.html. Last accessed: 09/2023.
- [14] Switch-IB™ 2 EDR Switch Silicon. <https://network.nvidia.com/files/doc-2020/pb-switchib2-edr-switch-silicon.pdf>. Last accessed: 09/2023.
- [15] Criteo: Terabyte Click Logs Dataset. <https://labs.criteo.com/2013/12/download-terabyte-click-logs>, 2013.
- [16] ABADI, M., AGARWAL, A., BARHAM, P., BREVDO, E., CHEN, Z., CITRO, C., CORRADO, G. S., DAVIS, A., DEAN, J., DEVIN, M., ET AL. Tensorflow: Large-scale Machine Learning on Heterogeneous Distributed Systems. *arXiv preprint arXiv:1603.04467* (2016).
- [17] ABRAMSON, D., JACKSON, J., MUTHRASANALLUR, S., NEIGER, G., REGNIER, G., SANKARAN, R., SCHOINAS, I., UHLIG, R., VEMBU, B., AND WIEGERT, J. Intel Virtualization Technology for Directed I/O. *Intel technology journal* 10, 3 (2006).
- [18] ALISTARH, D., GRUBIC, D., LI, J., TOMIOKA, R., AND VOJNOVIC, M. QSGD: Communication-efficient SGD via Gradient Quantization and Encoding. *NeurIPS* (2017).
- [19] ALIZADEH, M., GREENBERG, A., MALTZ, D. A., PADHYE, J., PATEL, P., PRABHAKAR, B., SENGUPTA, S., AND SRIDHARAN, M. Data Center TCP (DCTCP). In *ACM SIGCOMM* (2010).
- [20] ANANTHANARAYANAN, G., GHODSI, A., SHENKER, S., AND STOICA, I. Effective Straggler Mitigation: Attack of the Clones. In *USENIX NSDI* (2013).
- [21] BAI, Y., LI, C., ZHOU, Q., YI, J., GONG, P., YAN, F., CHEN, R., AND XU, Y. Gradient Compression Supercharged High-performance Data Parallel DNN Training. In *ACM SIGOPS* (2021).
- [22] BARAK, D. RDMA Aware Networks Programming User Manual. *NVIDIA Docs* (2015).
- [23] BOTTOU, L. Stochastic gradient descent tricks. *Neural Networks: Tricks of the Trade: Second Edition* (2012).
- [24] BROWN, T., MANN, B., RYDER, N., SUBBIAH, M., KAPLAN, J. D., DHARIWAL, P., NEELAKANTAN, A., SHYAM, P., SASTRY, G., ASKELL, A., ET AL. Language Models are Few-shot Learners. *NeurIPS* (2020).
- [25] CHEN, J., PAN, X., MONGA, R., BENGIO, S., AND JOZEFOWICZ, R. Revisiting Distributed Synchronous SGD. *arXiv preprint arXiv:1604.00981* (2016).
- [26] CHEN, T., LI, M., LI, Y., LIN, M., WANG, N., WANG, M., XIAO, T., XU, B., ZHANG, C., AND ZHANG, Z. Mxnet: A Flexible and Efficient Machine Learning Library for Heterogeneous Distributed Systems. *arXiv preprint arXiv:1512.01274* (2015).
- [27] CHO, K., VAN MERRIËNBOER, B., GULCEHRE, C., BAHDANAU, D., BOUGARES, F., SCHWENK, H., AND BENGIO, Y. Learning Phrase Representations Using RNN Encoder-Decoder for Statistical Machine Translation. *arXiv preprint arXiv:1406.1078* (2014).
- [28] CIPAR, J., HO, Q., KIM, J. K., LEE, S., GANGER, G. R., GIBSON, G., KEETON, K., AND P XING, E. Solving the straggler problem with bounded staleness. *White paper, Carnegie Mellon University* (2013).
- [29] CLARKE, L., GLENDINNING, I., AND HEMPEL, R. The MPI Message Passing Interface Standard. In *Programming Environments for Massively Parallel Distributed Systems, Springer* (1994).
- [30] CRANKSHAW, D., WANG, X., ZHOU, G., FRANKLIN, M. J., GONZALEZ, J. E., AND STOICA, I. Clipper: A Low-Latency Online Prediction Serving System. In *USENIX NSDI* (2017).
- [31] DEAN, J., AND BARROSO, L. A. The Tail at Scale. *Communications of the ACM* 56, 2 (2013).
- [32] DEAN, J., CORRADO, G., MONGA, R., CHEN, K., DEVIN, M., MAO, M., RANZATO, M., SENIOR, A., TUCKER, P., YANG, K., ET AL. Large Scale Distributed Deep Networks. *NeurIPS* (2012).
- [33] DENG, J., DONG, W., SOCHER, R., LI, L.-J., LI, K., AND FEI-FEI, L. Imagenet: A Large-Scale Hierarchical Image Database. In *IEEE CCVPR* (2009).
- [34] DEVLIN, J., CHANG, M.-W., LEE, K., AND TOUTANOVA, K. Bert: Pre-training of Deep Bidirectional Transformers for Language Understanding. *arXiv preprint arXiv:1810.04805* (2018).
- [35] DU, X., EL-KHAMY, M., LEE, J., AND DAVIS, L. Fused DNN: A Deep Neural Network Fusion Approach to Fast and Robust Pedestrian Detection. In *IEEE winter conference on applications of computer vision (WACV)* (2017).
- [36] DUTTA, S., JOSHI, G., GHOSH, S., DUBE, P., AND NAGPURKAR, P. Slow and Stale Gradients Can Win The Race: Error-runtime Trade-offs in Distributed SGD. In *International conference on artificial intelligence and statistics* (2018).
- [37] FEI, J., HO, C.-Y., SAHU, A. N., CANINI, M., AND SAPIO, A. Efficient Sparse Collective Communication and its Application to Accelerate Distributed Deep Learning. In *ACM SIGCOMM* (2021).
- [38] FEI, X., JIANIAN, X., JIABIN, C., LI, C., RUITAO, S., ZHI, Z., AND FANGMING, L. iGniter: Interference-Aware GPU Resource Provisioning for Predictable DNN Inference in the Cloud. *arXiv preprint arXiv:2211.01713* (2022).
- [39] FENG, S., ZHOU, H., AND DONG, H. Using Deep Neural Network with Small Dataset to Predict Material Defects. *Materials & Design* 162 (2019).
- [40] FINO, B. J., AND ALGAZI, V. R. Unified Matrix Treatment of the Fast Walsh-Hadamard Transform. *IEEE Transactions on Computers* 25, 11 (1976).
- [41] FU, M., QU, H., YI, Z., LU, L., AND LIU, Y. A Novel Deep Learning-based Collaborative Filtering Model for Recommendation System. *IEEE transactions on cybernetics* 49, 3 (2018).
- [42] GEBARA, N., GHOBADI, M., AND COSTA, P. In-network Aggregation for Shared Machine Learning Clusters. *MLSys* 3 (2021).
- [43] GHOBADI, J. S. A. S. M., AND MÉDARD, M. FlexEnt: Entropy Coding to Curb Stragglers in Large-Scale Distributed Machine Learning. *Workshop on AI Systems at SOSP* (2019).
- [44] GIBIANSKY, A. Bringing HPC Techniques to Deep Learning. *Baidu Research, Tech. Rep.* (2017).

- [45] GOEL, A., TUNG, C., LU, Y.-H., AND THIRUVATHUKAL, G. K. A Survey of Methods for Low-power Deep Learning and Computer Vision. In *IEEE 6th World Forum on Internet of Things (WF-IoT)* (2020).
- [46] GRAHAM, R. L., BUREDDY, D., LUI, P., ROSENSTOCK, H., SHAINER, G., BLOCH, G., GOLDENERG, D., DUBMAN, M., KOTCHUBIEVSKY, S., KUSHNIR, V., ET AL. Scalable Hierarchical Aggregation Protocol (SHArP): A Hardware Architecture for Efficient Data Reduction. In *IEEE International Workshop on Communication Optimizations in HPC (COMHPC)* (2016).
- [47] GUO, C., WU, H., DENG, Z., SONI, G., YE, J., PADHYE, J., AND LIPSHTEYN, M. RDMA over Commodity Ethernet at Scale. In *ACM SIGCOMM* (2016).
- [48] GUPTA, S., AGRAWAL, A., GOPALAKRISHNAN, K., AND NARAYANAN, P. Deep Learning with Limited Numerical Precision. In *ICML* (2015).
- [49] HARLAP, A., CUI, H., DAI, W., WEI, J., GANGER, G. R., GIBBONS, P. B., GIBSON, G. A., AND XING, E. P. Addressing the Straggler Problem for Iterative Nonconvergent Parallel ML. In *ACM Symposium on Cloud Computing* (2016).
- [50] HE, K., ZHANG, X., REN, S., AND SUN, J. Deep Residual Learning for Image Recognition. In *IEEE CCVPR* (2016).
- [51] HEREDIA, B., PRUSA, J. D., AND KHOSHGOFTAAR, T. M. Social Media for Polling and Predicting United States Election Outcome. *Social Network Analysis and Mining* 8, 1 (2018).
- [52] HOCHREITER, S., AND SCHMIDHUBER, J. Long Short-Term Memory. *Neural computation* 9, 8 (1997).
- [53] HUANG, Z., SHAN, G., CHENG, J., AND SUN, J. TRec: An Efficient Recommendation System for Hunting Passengers with Deep Neural Networks. *Neural Computing and Applications* 31, 1 (2019).
- [54] JIANG, Y., ZHU, Y., LAN, C., YI, B., CUI, Y., AND GUO, C. A Unified Architecture for Accelerating Distributed DNN Training in Heterogeneous GPU/CPU Clusters. In *USENIX OSDI* (2020).
- [55] JOSUTTIS, N. M. The C++ Standard Library: A Tutorial and Reference. Addison-Wesley (2012).
- [56] JOUPEI, N. P., YOUNG, C., PATIL, N., PATTERSON, D., AGRAWAL, G., BAJWA, R., BATES, S., BHATIA, S., BODEN, N., BORCHERS, A., ET AL. In-Datacenter Performance Analysis of a Tensor Processing Unit. In *ISCA* (2017).
- [57] KARAKUS, C., HUILGOL, R., WU, F., SUBRAMANIAN, A., DANIEL, C., CAVDAR, D., XU, T., CHEN, H., RAHMANA, A., AND QUINTELA, L. Amazon Sagemaker Model Parallelism: A General and Flexible Framework for Large Model Training. *arXiv preprint arXiv:2111.05972* (2021).
- [58] KARAKUS, C., SUN, Y., DIGGAVI, S., AND YIN, W. Straggler Mitigation in Distributed Optimization through Data Encoding. *NeurIPS* (2017).
- [59] KHAN, A. I., SHAH, J. L., AND BHAT, M. M. CoroNet: A Deep Neural Network for Detection and Diagnosis of COVID-19 from Chest X-Ray Images. *Computer methods and programs in biomedicine* 196 (2020).
- [60] KIEFER, J., AND WOLFOWITZ, J. Stochastic Estimation of The Maximum of a Regression Function. *The Annals of Mathematical Statistics* (1952).
- [61] KIM, S., YU, G.-I., PARK, H., CHO, S., JEONG, E., HA, H., LEE, S., JEONG, J. S., AND CHUN, B.-G. Parallax: Sparsity-aware Data Parallel Training of Deep Neural Networks. In *EuroSys* (2019).
- [62] KO, M., EISENHAEUER, D., AND RECIO, R. A Case for Convergence Enhanced Ethernet: Requirements and Applications. In *IEEE International Conference on Communications* (2008).
- [63] KOHLER, E., HANDLEY, M., AND FLOYD, S. Datagram congestion control protocol (DCCP). *RFC 4340* (2006).
- [64] KOZIARSKI, M., AND CYGANEK, B. Image Recognition with Deep Neural Networks in Presence of Noise—Dealing with and Taking Advantage of Distortions. *Integrated Computer-Aided Engineering* 24, 4 (2017).
- [65] KRIZHEVSKY, A., HINTON, G., ET AL. Learning Multiple Layers of Features from Tiny Images. *White paper, University of Toronto* (2009).
- [66] KRIZHEVSKY, A., SUTSKEVER, I., AND HINTON, G. E. Imagenet Classification with Deep Convolutional Neural Networks. *Communications of the ACM* 60, 6 (2017).
- [67] LAO, C., LE, Y., MAHAJAN, K., CHEN, Y., WU, W., AKELLA, A., AND SWIFT, M. M. ATP: In-network Aggregation for Multi-tenant Learning. In *USENIX NSDI* (2021).
- [68] LECUN, Y., ET AL. LeNet-5, Convolutional Neural Networks. URL: <http://yann.lecun.com/exdb/lenet>, 5 (2015).
- [69] LI, H., KADAV, A., KRUS, E., AND UNGUREANU, C. Malt: Distributed Data-Parallelism for Existing ML Applications. In *European Conference on Computer systems* (2015).
- [70] LI, M., ANDERSEN, D. G., SMOLA, A. J., AND YU, K. Communication Efficient Distributed Machine Learning with the Parameter Server. *NeurIPS* 27 (2014).
- [71] LI, M., ZHOU, L., YANG, Z., LI, A., XIA, F., ANDERSEN, D. G., AND SMOLA, A. Parameter Server for Distributed Machine Learning. In *Big learning NIPS workshop* (2013).
- [72] LI, S., ZHAO, Y., VARMA, R., SALPEKAR, O., NOORDHUIS, P., LI, T., PASZKE, A., SMITH, J., VAUGHAN, B., DAMANIA, P., ET AL. Pytorch Distributed: Experiences on Accelerating Data Parallel Training. *arXiv preprint arXiv:2006.15704* (2020).
- [73] LI, Y., LIU, I.-J., YUAN, Y., CHEN, D., SCHWING, A., AND HUANG, J. Accelerating Distributed Reinforcement Learning with In-switch Computing. In *ACM/IEEE ISCA* (2019).
- [74] LIN, Y., HAN, S., MAO, H., WANG, Y., AND DALLY, W. J. Deep Gradient Compression: Reducing the Communication Bandwidth for Distributed Training. *arXiv preprint arXiv:1712.01887* (2017).
- [75] LIU, X., HE, P., CHEN, W., AND GAO, J. Multi-task Deep Neural Networks for Natural Language Understanding. *arXiv preprint arXiv:1901.11504* (2019).
- [76] LOCKWOOD, J. W., MCKEOWN, N., WATSON, G., GIBB, G., HARTKE, P., NAOUS, J., RAGHURAMAN, R., AND LUO, J. NetFPGA—An Open Platform for Gigabit-Rate Network Switching and Routing. In *IEEE International Conference on Microelectronic Systems Education (MSE)* (2007).
- [77] MALICK, P. K., RYU, S. H., SATAPATHY, S. K., MISHRA, S., NGUYEN, G. N., AND TIWARI, P. Brain MRI Image Classification for Cancer Detection using Deep Wavelet Autoencoder-Based Deep Neural Network. *IEEE Access* 7 (2019).
- [78] MIKOLOV, T., KARAFIÁT, M., BURGET, L., CERNOCKÝ, J., AND KHUDANPUR, S. Recurrent Neural Network based Language Model. In *Interspeech* (2010).
- [79] MORITZ, P., NISHIHARA, R., STOICA, I., AND JORDAN, M. I. Sparknet: Training Deep Networks in Spark. *arXiv preprint arXiv:1511.06051* (2015).
- [80] MURRAY, D. G., MCSHERRY, F., ISAACS, R., ISARD, M., BARHAM, P., AND ABADI, M. Naiad: A timely Dataflow System. In *ACM SOSP* (2013).
- [81] NARAYANAN, D., HARLAP, A., PHANISHAYEE, A., SESHADRI, V., DEVANUR, N. R., GANGER, G. R., GIBBONS, P. B., AND ZAHARIA, M. PipeDream: Generalized Pipeline Parallelism for DNN Training. In *ACM SOSP* (2019).
- [82] OUYANG, X., WANG, C., AND XU, J. Mitigating Stragglers to Avoid QoS Violation for Time-critical Applications through Dynamic Server Blacklisting. *Future Generation Computer Systems* 101 (2019).
- [83] PATARASUK, P., AND YUAN, X. Bandwidth Optimal All-reduce Algorithms for Clusters of Workstations. *Journal of Parallel and Distributed Computing* 69, 2 (2009).
- [84] PAULY, T., KINNEAR, E., AND SCHINAZI, D. An Unreliable Datagram Extension to QUIC. *RFC 9221* (2022).
- [85] PETRINI, F., KERBYSON, D. J., AND PAKIN, S. The Case of the Missing Supercomputer Performance: Achieving Optimal Performance on the

- 8,192 Processors of ASCI Q. In *ACM/IEEE Conference on Supercomputing* (2003).
- [86] PFISTER, G. F. An Introduction to the Infiniband Architecture. *High performance mass storage and parallel I/O* 42, 617-632 (2001).
- [87] QI, Y., GUO, Y., AND WANG, Y. Image Quality Enhancement using a Deep Neural Network for Plane Wave Medical Ultrasound Imaging. *IEEE Transactions on Ultrasonics, Ferroelectrics, and Frequency Control* (2020).
- [88] RAJPURKAR, P., JIA, R., AND LIANG, P. Know What You Don't Know: Unanswerable Questions for SQuAD. *arXiv preprint arXiv:1806.03822* (2018).
- [89] RAMESH, S., YAASHUWANTH, C., PRATHIBANANDHI, K., BASHA, A. R., AND JAYASANKAR, T. An Optimized Deep Neural Network based DoS Attack Detection in Wireless Video Sensor Network. *Journal of Ambient Intelligence and Humanized Computing* (2021).
- [90] RENGGLI, C., ASHKBOOS, S., AGHAGOLZADEH, M., ALISTARH, D., AND HOEFLER, T. Sparcml: High-performance Sparse Communication for Machine Learning. In *Proceedings of the International Conference for High Performance Computing, Networking, Storage and Analysis* (2019).
- [91] RIGAZZI, A. DC-S3GD: Delay-Compensated Stale-Synchronous SGD for Large-Scale Decentralized Neural Network Training. In *ACM/IEEE Third Workshop on Deep Learning on Supercomputers (DLS)* (2019).
- [92] ROMERO, J., YIN, J., LAANAIT, N., XIE, B., YOUNG, M. T., TREICHLER, S., STARCHENKO, V., BORISEVICH, A., SERGEEV, A., AND MATHESON, M. Accelerating Collective Communication in Data Parallel Training across Deep Learning Frameworks. In *USENIX NSDI* (2022).
- [93] RUCKER, A., SHAHBAZ, M., AND OLUKOTUN, K. Chopping off the Tail: Bounded Non-Determinism for Real-Time Accelerators. *IEEE Computer Architecture Letters (CAL)* (2021).
- [94] SAPIO, A., CANINI, M., HO, C.-Y., NELSON, J., KALNIS, P., KIM, C., KRISHNAMURTHY, A., MOSHREEF, M., PORTS, D., AND RICHTÁRIK, P. Scaling Distributed Machine Learning with In-Network Aggregation. In *USENIX NSDI* (2021).
- [95] SHAH, A., CHIDAMBARAM, V., COWAN, M., MALEKI, S., MUSUVATHI, M., MYTKOWICZ, T., NELSON, J., SAARIKIVI, O., AND SINGH, R. TACCL: Guiding Collective Algorithm Synthesis using Communication Sketches. In *USENIX NSDI* (2023).
- [96] SIMONYAN, K., AND ZISSERMAN, A. Very Deep Convolutional Networks for Large-scale Image Recognition. *arXiv preprint arXiv:1409.1556* (2014).
- [97] STEINKRAUS, D., BUCK, I., AND SIMARD, P. Using GPUs for Machine Learning Algorithms. In *IEEE ICDAR* (2005).
- [98] SUN, C., SHRIVASTAVA, A., SINGH, S., AND GUPTA, A. Revisiting Unreasonable Effectiveness of Data in Deep Learning Era. In *IEEE ICCV* (2017).
- [99] SURESH, A. T., FELIX, X. Y., KUMAR, S., AND McMAHAN, H. B. Distributed Mean Estimation with Limited Communication. In *ICML* (2017).
- [100] TANDON, R., LEI, Q., DIMAKIS, A. G., AND KARAMPATZIAKIS, N. Gradient Coding: Avoiding Stragglers in Distributed Learning. In *ICML* (2017).
- [101] TOUVRON, H., LAVRIL, T., IZACARD, G., MARTINET, X., LACHAUX, M.-A., LACROIX, T., ROZIÈRE, B., GOYAL, N., HAMBRO, E., AZHAR, F., ET AL. Llama: Open and Efficient Foundation Language Models. *arXiv preprint arXiv:2302.13971* (2023).
- [102] VARGAFTIK, S., BASAT, R. B., PORTNOY, A., MENDELSON, G., ITZHAK, Y. B., AND MITZENMACHER, M. Eden: Communication-efficient and Robust Distributed Mean Estimation for Federated Learning. In *ICML* (2022).
- [103] VARGAFTIK, S., BEN-BASAT, R., PORTNOY, A., MENDELSON, G., BEN-ITZHAK, Y., AND MITZENMACHER, M. Drive: One-bit Distributed Mean Estimation. *NeurIPS* (2021).
- [104] VASWANI, A., SHAZEER, N., PARMAR, N., USZKOREIT, J., JONES, L., GOMEZ, A. N., KAISER, L., AND POLOSUKHIN, I. Attention is All You Need. *NeurIPS* (2017).
- [105] VISWANATHAN, R., BALASUBRAMANIAN, A., AND AKELLA, A. Network-accelerated Distributed Machine Learning for Multi-tenant Settings. In *ACM Symposium on Cloud Computing* (2020).
- [106] WANG, H., CHEN, J., WAN, X., TIAN, H., XIA, J., ZENG, G., WANG, W., CHEN, K., BAI, W., AND JIANG, J. Domain-specific Communication Optimization for Distributed DNN Training. *arXiv preprint arXiv:2008.08445* (2020).
- [107] WANGNI, J., WANG, J., LIU, J., AND ZHANG, T. Gradient Sparsification for Communication-efficient Distributed Optimization. *arXiv preprint arXiv:1710.09854* (2017).
- [108] WEN, W., XU, C., YAN, F., WU, C., WANG, Y., CHEN, Y., AND LI, H. Terngrad: Ternary Gradients to Reduce Communication in Distributed Deep Learning. *NeurIPS* (2017).
- [109] WILLIAMS, S., WATERMAN, A., AND PATTERSON, D. Roofline: An Insightful Visual Performance Model for Multicore Architectures. *Communications of the ACM* 52, 4 (2009).
- [110] XAVIER, B. M., GUIMARÃES, R. S., COMARELA, G., AND MARTINELLO, M. Programmable Switches for In-Network Classification. In *IEEE INFOCOM* (2021).
- [111] XIA, J., ZENG, G., ZHANG, J., WANG, W., BAI, W., JIANG, J., AND CHEN, K. Rethinking Transport Layer Design for Distributed Machine Learning. In *APNet* (2019).
- [112] XIAO, H., RASUL, K., AND VOLLGRAF, R. Fashion-MNIST: A Novel Image Dataset for Benchmarking Machine Learning Algorithms. *arXiv preprint arXiv:1708.07747* (2017).
- [113] XIONG, G., YAN, G., SINGH, R., AND LI, J. Straggler-resilient Distributed Machine Learning with Dynamic Backup Workers. *arXiv preprint arXiv:2102.06280* (2021).
- [114] XIONG, Z., AND ZILBERMAN, N. Do Switches Dream of Machine Learning? Toward In-Network Classification. In *ACM HotNets* (2019).
- [115] XU, C., CHAI, D., HE, J., ZHANG, X., AND DUAN, S. InnoHAR: A Deep Neural Network for Complex Human Activity Recognition. *IEEE Access* 7 (2019).
- [116] XU, Y., MUSGRAVE, Z., NOBLE, B., AND BAILEY, M. Bobtail: Avoiding Long Tails in the Cloud. In *USENIX NSDI* (2013).
- [117] YADWADKAR, N. J., AND CHOI, W. Proactive Straggler Avoidance using Machine Learning. *White paper, University of Berkeley* (2012).
- [118] YAKIMENKA, Y., WENG, C.-W., LIN, H.-Y., ROSNES, E., AND KIEWER, J. Straggler-Resilient Differentially-Private Decentralized Learning. In *IEEE Information Theory Workshop (ITW)* (2022).
- [119] YIN, W., KANN, K., YU, M., AND SCHÜTZE, H. Comparative Study of CNN and RNN for Natural Language Processing. *arXiv preprint arXiv:1702.01923* (2017).
- [120] YUAN, X., LI, W., LIN, K., AND HU, J. A Deep Neural Network Based Hierarchical Multi-Label Classifier for Protein Function Prediction. In *International Conference on Computer, Information and Telecommunication Systems (CITS)* (2019).
- [121] ZERVAKIS, G., SAADAT, H., AMROUCH, H., GERSTLAUER, A., PARAMESWARAN, S., AND HENKEL, J. Approximate Computing for ML: State-of-the-Art, Challenges and Visions. In *ACM ASPDAC* (2021).
- [122] ZHANG, H., ZHENG, Z., XU, S., DAI, W., HO, Q., LIANG, X., HU, Z., WEI, J., XIE, P., AND XING, E. P. Poseidon: An Efficient Communication Architecture for Distributed Deep Learning on GPU Clusters. In *USENIX ATC* (2017).
- [123] ZHANG, Z., LI, C., TAO, Y., YANG, R., TANG, H., AND XU, J. Fuxi: A Fault-tolerant Resource Management and Job Scheduling System at Internet Scale. In *Proceedings of the VLDB Endowment* (2014).

- [124] ZINKEVICH, M., WEIMER, M., LI, L., AND SMOLA, A. Parallelized Stochastic Gradient Descent. *NeurIPS* (2010).